First-Principles Investigation of Surface and Subsurface H Adsorption on Ir(111)

Hong Zhang and Wei-Xue Li*

School of Physical Science and Technology, Sichuan University, Chengdu 610065, China, and State Key Laboratory of Catalysis, Dalian Institute of Chemical Physics, Chinese Academy of Sciences, Dalian 116023, China

The atomic hydrogen adsorption on Ir (111) surface and in its subsurface with coverage from 0.11 monolayer (ML) to 2 ML is investigated by using density functional calculations with the generalized gradient approximation (GGA), the diffusion for hydrogen into the subsurface region at 0.25 ML coverage is also calculated. At all sites of our calculations, the most favorable site is hydrogen on top of Ir (111). The corresponding binding energy of a hydrogen atom at this site is 2.71 eV/H atom at the coverage of 0.25 ML, favored by about 0.05 eV over the next most stable site, the fcc site. For on-surface adsorption, the binding energy decreases very slowly for all of the sites as the hydrogen coverage increases from 0.25 to 1.00 ML, it indicates that there is only a weak repulsive interaction between the adsorbates. For the coverage range of 0.11−0.25 ML, the binding energy increases evidently, suggesting an attractive interaction between adsorbates. Compared to on-surface hydrogen adsorption, subsurface hydrogen adsorption is energetically unfavorable and takes place when on-surface hydrogen coverage is greater than full monolayer. For mixed structures at full monolayer both of surface and subsurface, it is found that the most favorable site is the hcp/octa site with a binding energy 2.35 eV/H atom. So when full monolayer hydrogen atoms adsorbed in the hcp site on the surface, H begins to adsorb on the subsurface in the octa site. Compared to hydrogen adsorption on other transition metals (Pt, Rh, Pd, Co, and Ni) with localized feature, it is found hydrogen adsorption on Ir (111) shows some delocalized nature. Meanwhile, at 0.25 ML coverage for H adsorption on Ir(111), the desorption energy for hydrogen from the Ir surface is found to be 0.96 eV, the calculated barrier for hydrogen from hcp to fcc is 0.02 eV, and penetration into the subsurface region from the on surface fcc site is 1.26 eV.

1. Introduction

Because of its nonpolluting nature, hydrogen is considered to be an ideal fuel of the future, and it is expected to be a key component in solving the energy crisis as well as minimizing environmental impact. The interaction between hydrogen and metals is important for production of many chemicals and hydrogen storage technologies.[1] Some reports pay more attention to the nature of hydrogen adsorption on metal surfaces because hydrogen is regarded as a key intermediate for catalytic reactions, also transition metals are important for heterogeneous catalysts for a wide range of hydrocarbon transformations, and many investigations about the behavior of their surface have been done both experimentally and theoretically.[2] As a late 5d transition metal, iridium shows potential in a great variety of applications, particularly as a heterogeneous catalyst in various industrial chemical reactions.[3] Ir and Ir-alloy catalysts are widely used in reactions that require the activation of strong C−H bonds. Clearly, a more detailed atomic-level understanding of the interactions of hydrogen with Ir surfaces would be very valuable, which could lead to improved Ir-based catalysts with greater selectivity and activity.[4] Hence, some studies have been made on hydrogen adsorption on iridium surface,[5] and a wide range of different effects such as the existence of different adsorption phases and the penetration of hydrogen into the near-surface region and oxide iridium were studied for iridium and other transition metals.[6] These topics are necessary to understand the reactivity of the transition-metal surface in various catalytic reactions, and it cannot be investigated experimentally in such

a direct way as it is for other atoms because of the low electron density around the hydrogen atom center.[7] Being the lightest atom also gives rise to the high mobility of the hydrogen atom on the surface, quantum effects, etc. Studies of hydrogen adsorption on pure transition metals are also important for understanding the process of transition metal hydride formation. The H/Cu(111), H/Pd(111), H/Pt(111),[8] H/Ag(111),[9] H/Rh-(111),[10] and H/Ni(111)[11] systems have been studied in detail. Greeley et al. report the thermochemical properties of both surface and subsurface atomic hydrogen on a variety of pure metals and near-surface alloys.[12] Experimental and theoretical studies on the quantum delocalization of hydrogen atoms, in particular in vibrationally excited states, on transition-metal surfaces are also performed.[13] Hagedorn et al.[14] studied the dissociative chemisorption of hydrogen on the Ir(111) surface and found evidence for terminal site adsorption. Absence of a significant isotopic energy shift for the parallel mode was found in the vibrational spectra for low coverage of H and D and was interpreted to be indicative of the quantum delocalized motion of hydrogen.

To the best of our knowledge, there is no systematic study on hydrogen adsorption on the Ir(111) surface at wide coverage, especially lower than 0.25 ML and higher than 1.00 ML. Meanwhile, it is important to study the behaviors of hydrogen atoms on the Ir surface and in the subsurface in detail, such as the adsorption and the diffusion of hydrogen atoms. Because of the small mass of the hydrogen, it is also necessary to consider the localized nature or not in investigating the behavior of the hydrogen atom on the surface of Ir. These depend on the curvature of the potential energy surface for the hydrogen atom

* Corresponding author. E-mail: wxli@dicp.ac.cn.

TABLE 1: Average Binding Energy $E_b^{H/Ir}$ (eV/H Atom) for H on the Ir(111) Surface at the Coverage from 0.11 to 1.00 ML[a]

								on-surface														
site		fcc							hcp					top					bridge		
θ(ML)		0.11	0.25	0.33	0.50	0.67	0.75	1.00	0.11	0.25	0.50	0.75	1.00	0.11	0.25	0.50	0.75	1.00	0.25	0.50	1.00
$E_b^{H/Ir}$	present	1.97	2.66	2.63	2.64	2.60	2.62	2.60	1.96	2.65	2.63	2.60	2.58	2.02	2.71	2.68	2.66	2.65	2.63	2.58	2.33
	others[c]		2.62[b]	2.67[c]		2.64[c]		2.62[c]					2.57[b]	2.74[b]				2.68[c]			2.58[c]
				(exp 2.52[b])																	
H	present	1.05	1.01	1.04	1.05	1.05	1.04	1.03	1.05	0.99	1.10	1.04	1.02	1.67	1.68	1.64	1.61	1.60	1.15	1.13	1.15
	others[c]		1.59[b]					1.04[c]					1.03[c]					1.59[c]			1.17[c]

[a] Adsorption height (h in Å) means the perpendicular distance of hydrogen to the plane of nearest-neighbor surface Ir atoms. [b] Reference 12. [c] Reference 2.

TABLE 2: Average Binding Energy $E_b^{H/Ir}$ (eV/H atom) for H in Subsurface of Ir(111) and Mix-Structures[a]

	subsurface						on-surface and subsurface							
site	tetra-I	tetra-II	octa				fcc(4)+tetra-I(1)	hcp(4)+octa(1)	fcc(4)+tetra-I(2)	hcp(4)+octa(2)	fcc(4)+tetra-I(3)	hcp(4)+octa(3)	fcc(4)+tetra-I(4)	hcp(4)+octa(4)
coverage	1.00	0.25	0.25	0.50	0.75	1.00	1.25		1.50		1.75		2.00	
$E_b^{H/Ir}$	1.53	1.25 (1.06[b])	1.55	1.52	1.52	1.56	2.32	2.35	2.21	2.21	2.15	2.28	2.12	2.06
h	0.92	1.37 (1.62[b])	0.46	0.74	0.86	0.92	0.99 (fcc) 0.67 (tetra1)	0.99 (hcp) 0.90 (octa)	0.86 (fcc) 0.82 (tetra1)	0.94 (hcp) 0.93 (octa)	0.74 (fcc) 0.81 (tetra1)	0.89 (hcp) 0.98 (octa)	0.92 (fcc) 0.96 (tetra1)	0.98 (hcp) 1.00 (octa)

[a] For the subsurface H, the adsorption height (h in Å) is the distance of H to the top layer of Ir atoms. [b] Reference 12.

motion. In this paper, we present atomic hydrogen adsorption on the surface and in the subsurface of Ir(111) for a wide range of hydrogen coverage, namely from 0.11 to 2.0 ML. We also calculate the adiabatic potential energy for hydrogen atom motion on the Ir(111) surface and in the subsurface, and a first-principles potential energy surface (PES) for hydrogen diffusion from the Ir(111) surface to the first subsurface and to the second subsurface layer at 0.25 ML for fcc and hcp site is also presented.

2. Calculation Method

In this study the density-functional theory calculations are performed using the Vienna ab initio simulation package VASP,[15] and the generalized-gradient approximation (GGA) using the Perdew−Wang (PW-91) for the exchange-correlation functional was employed.[16−18] The wave functions are expanded in a plane-wave basis set with an energy cutoff of 36.75 Ry (500 eV). The Ir(111) surface is modeled by a five-layer slab that is separated from its periodic images by a vacuum larger than 15 Å. Hydrogen is placed on one side of the slab. Atomic relaxation of all iridium atoms in the three topmost layers and the adsorbed hydrogen atoms are allowed, whereas the bottom two layers of the slab are held fixed. The Brillouin-zone integrations are performed using a (12 × 12 × 12) Monkhorst-Pack (MP) grid for bulk, and (6 × 6 × 1) MP grid for the Ir(111) surface using (2 × 2) unit cell, respectively. It is necessary that bulk and surface calculations are performed with the same high accuracy to obtain highly converged surface properties. The final forces on the atoms are less than 0.01 eV/Å. The average binding energy per hydrogen atom $E_b^{H/Ir}$ with respect to atomic hydrogen in gas phase is defined as[19,20]

$$E_b^{H/Ir} = -\frac{1}{N_H}[E^{H/Ir} - (E^{Ir} + N_H E^{H})] \qquad (1)$$

where N_H, $E^{H/Ir}$, E^{Ir}, and E^{H} are the number of hydrogen atoms in the surface unit cell, the total energies of the adsorbate−substrate system, the clean surface, and the hydrogen atom in gas phase, respectively. The positive (negative) values indicate the adsorption is exothermic (endothermic). For the electronic properties, the work-function change and projected density of

states are analyzed for hydrogen coverage on Ir(111), and the results are compared with H on other transition metal surfaces.

To study the hydrogen penetration into the subsurface and bulk region, we also calculate the corresponding potential energy surface of hydrogen on Ir(111) based on the rigid substrate approximation. The clean Ir(111) surface structure was used to represent the Ir(111) substrate, and Z coordinates are fixed in the direction perpendicular to the surface from +3.0 to −6.0 Å at an interval of 0.25 Å.

3. Results and Discussion

For the properties of bulk Ir and the Ir(111) surface, the calculated bulk lattice constant is 3.89 Å neglecting zero-point vibrations, and the bulk modulus is calculated to be 3.43 GPa, which are in good agreement with the corresponding experimental values of 3.84 Å and 3.55 GPa.[21] The calculated properties for the adsorption of hydrogen atom on surface and in subsurface of Ir(111) are listed in Tables 1 and 2. Regarding on-surface hydrogen adsorption, we calculate the binding energies for a range of coverage θ: (3 × 3)-H ($\theta = 0.11$ ML), θ: (3 × 3)-3H ($\theta = 0.33$ ML), θ: (3 × 3)-6H ($\theta = 0.67$ ML), (2 × 2)-H ($\theta = 0.25$ ML), (2 × 2)-2H ($\theta = 0.50$ ML), (2 × 2)-3H ($\theta = 0.75$ ML), and (2 × 2)-4H ($\theta = 1.00$ ML). The fcc, hcp hollow, top, and bridge sites are considered. For
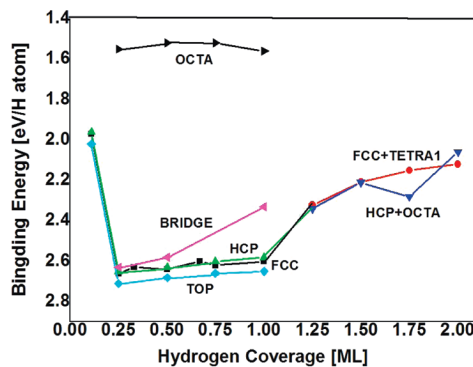

Figure 1. Average binding energy of hydrogen on Ir(111) for the on-surface, subsurface, and mixed structure (on-surface plus subsurface) sites for various coverage with respect to the energy of a hydrogen atom in gas phase.

Surface and Subsurface H Adsorption on Ir(111)

J. Phys. Chem. C, Vol. 113, No. 51, 2009 **21363**

TABLE 3: Calculated Structural Parameters (in Å) for Various Coverage of H in the Favorable Sites on Ir(111)[a]

sites	fcc							hcp					top					bridge		
coverage	0.11	0.25	0.33	0.50	0.67	0.75	1.00	0.11	0.25	0.50	0.75	1.00	0.11	0.25	0.50	0.75	1.00	0.25	0.50	1.00
d_{HIr}	3.606	3.603	3.511	3.508	3.518	3.474	3.567	3.592	3.548	3.410	3.401	3.560	3.018	3.026	3.021	3.018	3.016	3.393	3.379	3.348
d_{01}	1.049	1.005	1.038	1.046	1.049	1.041	1.028	1.048	0.989	1.099	1.041	1.018	1.668	1.679	1.636	1.608	1.596	1.154	1.129	1.145
d_{12}	2.219	2.215	2.239	2.231	2.259	2.246	2.255	2.221	2.220	2.240	2.260	2.279	2.212	2.217	2.219	2.214	2.212	2.213	2.230	2.270
d_{23}	2.243	2.238	2.236	2.240	2.252	2.242	2.236	2.242	2.236	2.234	2.231	2.227	2.240	2.251	2.257	2.262	2.268	2.237	2.239	2.240

[a] d_{HIr} is the bond length between hydrogen and the first-nearest-neighbor iridium atom, d_{01} is the H/Ir vertical height of hydrogen above the topmost iridium layer, and d_{12} and d_{23} are the first and second metal interlayer spacing, respectively, where the center of mass of the layer is used. The calculated interlayer distance for bulk iridium is 2.246 Å.

subsurface sites, we calculate adsorption in (i) the octahedral site, denoted hereafter as "octa", and (ii) the tetrahedral sites. There are two types of tetrahedral sites: one is where there are three Ir atoms above it and one below, denoted as tetra-I, and the alternative one, tetra-II, is just the opposite with one surface Ir atom directly above and three below it in the second Ir layer. For structures involving mix structure, both on-surface and subsurface hydrogen atoms, we start from the (2 × 2)-4H on-surface configuration and add subsurface hydrogen atoms below the first surface of Ir layer. Two possible site configurations, fcc/tetra-I, and hcp/octa, for various coverage are investigated, and calculations for hydrogen in these different sites up to a total coverage 2.0 ML were performed (see Figure 1).

For pure on-surface hydrogen adsorption at the coverage of 0.25 ML, see Table 1, H binds almost the same favorably to the fcc, hcp, and top sites with an adsorption energy in the range of 2.63−2.71 eV, and the top site is slightly more favorable by 0.05 eV than the fcc site. Moreover, it can be seen that the binding energy for H on Ir(111) decreases very slowly from 2.66 to 2.60 eV with the coverage increasing from $\theta = 0.25$ to 1.00 ML for fcc site, which indicates a weak lateral interaction between adsorbed H atoms. Our results are in good agreement with previous DFT studies[22] as well as with the experimental observation that H does not form an ordered overlayer structure at submonolayer coverage.[14] For the lower coverage 0.11 ML, compared to 0.25 ML, the binding energy decreases evidently, suggesting an attractive interaction between isolated adsorbates.

Table 2 is the binding energy for H in subsurface of Ir(111) and the mixed structures. From this table, we can know, for pure subsurface hydrogen adsorption at the coverage of from 0.25 to 1.00 ML, the most favorable adsorption site is octa site at 1.00 ML hydrogen coverage, with an average binding energy of 1.56 eV which is significantly smaller than the value of on-surface adsorption. We found that hydrogen in the tetra-I site is unstable until the 1.00 ML hydrogen coverage with the binding energy of 1.53 eV, whereas for hydrogen coverage at 0.25, 0.50, and 0.75 ML, the subsurface hydrogen atom diffuses upward to the surface without any barrier and occupies a hcp site. Compared to on-surface adsorption at the same coverage, these calculations show that the isolated subsurface H atom is energetically unfavorable, and H atoms prefer to adsorb on the surface. The same phenomena occurs in the tetra-II site, just 0.25 ML is stable with the binding energy of 1.25 eV. Though it is energetically unfavorable for H adsorption only at subsurface sites, it may coexist with on-surface hydrogen. Since there is no pronounced lateral repulsion between on-surface hydrogen and there is a large difference in the binding energy between on-surface and subsurface hydrogen, the formation of subsurface hydrogen will not take place until there is a full monolayer of hydrogen on the surface. Up to now, the clear knowledge of saturation coverage is still unreasonable experimentally because of the limited factors such as the resolution and device. We investigate the mix structures, namely on-surface plus subsurface, for hydrogen adsorption on Ir (111). With a full monolayer

of hydrogen atoms in the fcc site plus 0.25 ML subsurface hydrogen atom in the tetra-I sites, with the total hydrogen coverage up to $\theta = 1.25$ ML, the binding energy is 2.32 eV, and later it decreases gradually to 2.12 eV at $\theta = 2.00$ ML (with 1.00 ML hydrogen coverage in tetra-I). For the structure with the full monolayer H atoms in hcp sites plus octa in
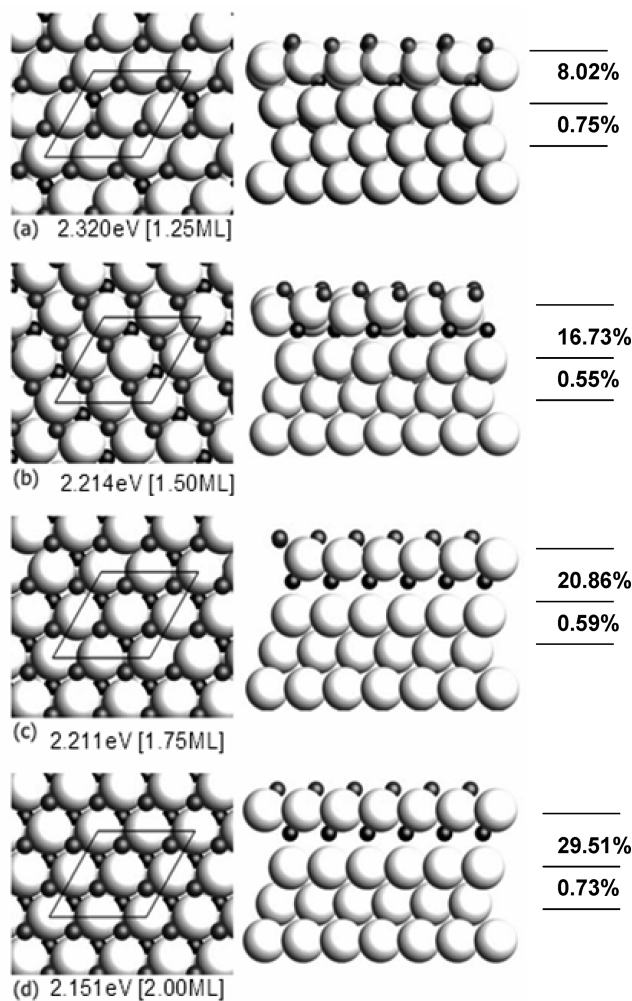

Figure 2. Atomic geometry of hydrogen structures with a full monolayer of hydrogen on the surface in the fcc site, for increasing subsurface hydrogen concentrations, as calculated using a (2 × 2) surface unit cell. (a) Full monolayer (four hydrogen atoms per (2 × 2) cell) plus one subsurface hydrogen atom in the tetra-I site, (b) as for (a) but with two hydrogen atoms in the tetra-I site, and (c and d) as for (b) but with three and four hydrogen atoms in the tetra-I site, respectively. The average binding energy as well as the corresponding coverage is given at the bottom of each panel. The relative variation of the metal interlayer spacings, with respect to the bulk value, is given to the right of the figures. The large and small spheres represent iridium and hydrogen atoms, respectively.
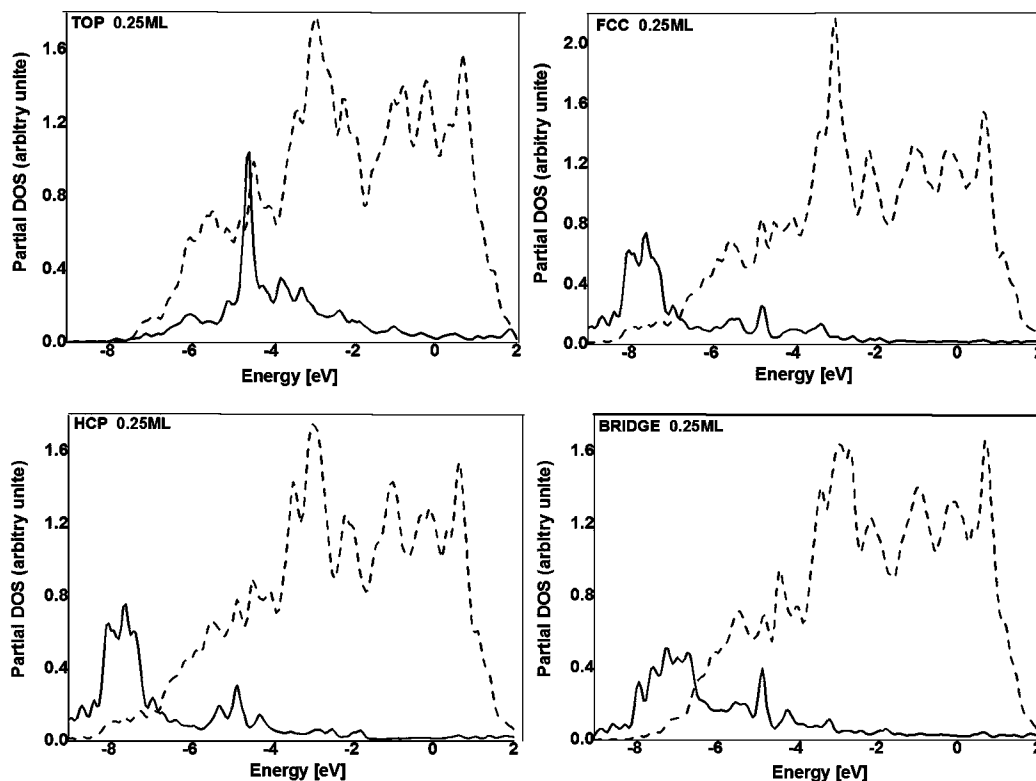
Figure 3. Projected density of states (PDOS) for the pure on-surface H atom (solid lines) and surface Ir atom (dash lines) with 0.25 ML at the fcc, hcp, top, and bridge sites. The energy reference is the Fermi level.
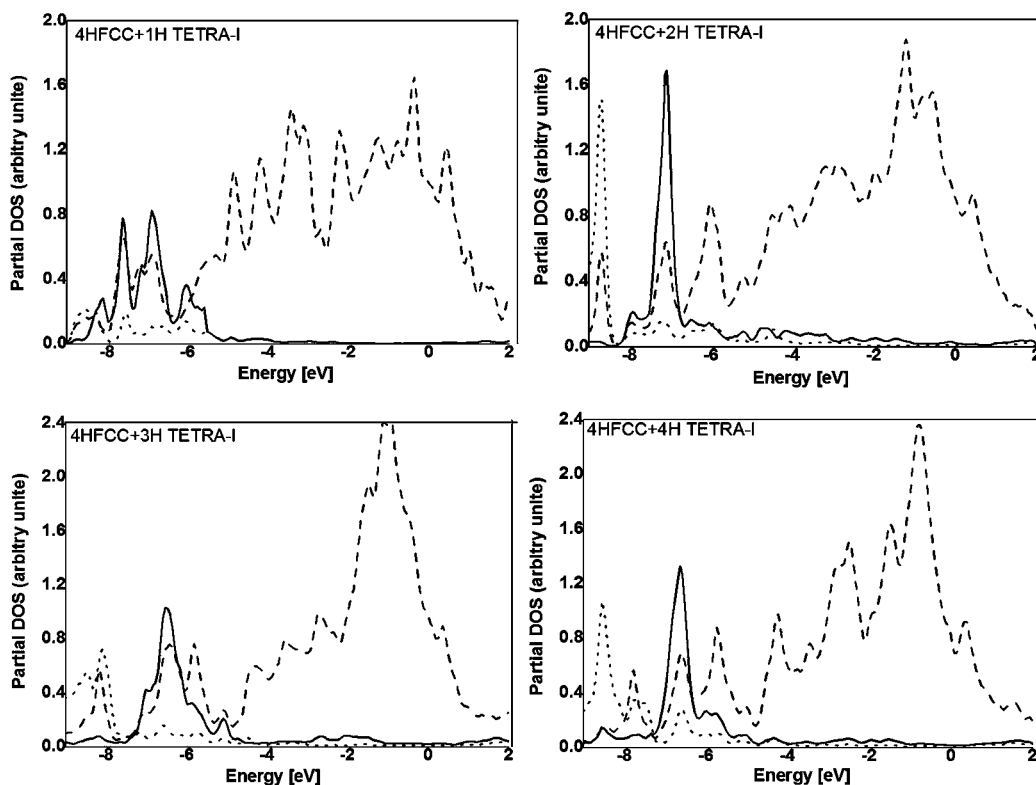

Figure 4. PDOS for the on-surface (solid lines) and subsurface H atom (dot lines) and surface Ir atom (dash lines) for the fcc/tetra-I configuration at overall coverage 1.25 ML (4H FCC+1H TETRA-I), 1.50 ML (4H FCC+2HTETRA-I), 1.75 ML (4H FCC+3H TETRA-I), and 2.00 ML (4H FCC+4H TETRA-I).

subsurface, a similar trend has been found except for the structure at total coverage 1.75 ML, which shows a more stable character.

Up to now, it is appropriate to make a comparison between our result and other calculations. Recently, Ferrin et al.[23] reported

that the binding energy of H on Ir(111) is 2.73 eV at the top site for 0.25 ML coverage, this value is very close to ours 2.71 eV. At a different coverage of hydrogen, the results of our calculations are in good agreement with those of Faglioni and Goddard[2] listed in Table 1. At 1/3 ML coverage at the fcc site,

Surface and Subsurface H Adsorption on Ir(111)

J. Phys. Chem. C, Vol. 113, No. 51, 2009 **21365**

the experiment data of the binding energy is 2.52 eV (58.1 kcal/mol), ours is 2.63 eV, and Faglioni and Goddard's is 2.67 eV. From ref 2, the zero-point energy (ZPE) for H/Ir(111) at 1/3 ML is approximately 0.08 eV, if we use such ZPE to correct the binding energy, our corrected value should be 2.55 eV.

The calculated atomic geometries of the H/Ir(111) structures (for $\theta = 0.11-1$ ML, adsorption on pure surface) are listed in Table 3. The relaxed metal interlayer distances d_{12} and d_{23} for the clean Ir(111) surface are 2.198 and 2.241 Å, respectively, and the interlayer distance for bulk Ir is 2.246 Å. The calculated contractions 2.1% for d_{12} and 0.6% for d_{23} agree well with experimental values 2.1% and 0.6%, respectively.[6,24] For hydrogen adsorption on Ir (111) at a coverage of 0.11 ML at the top site, i.e., the most favorable site, the metal interlayer distances are 2.219 and 2.243 Å, showing an expansion of 0.95% for d_{12} relative to the clean surface and almost no expansion for the second interlayer distance. For the coverage of 0.25 ML at the top site, the metal interlayer distances are 2.217 and 2.251 Å, showing an expansion of 0.86% for d_{12} relative to the clean surface, and 0.46% for the second interlayer distance. With the coverage increasing, the expansion of the topmost metal interlayer decreases slightly, and the expansion is about 0.63% at the coverage of 1.00 ML. As for the fcc adsorption site at the lowest coverage (0.11 ML) within our calculation, d_{12} and d_{23} are 2.219 and 2.243 Å. The expansion is 0.96% for the topmost metal interlayer, and it decreases to 0.77% when hydrogen coverage is 0.25 ML. After that, from 0.25 to 1.00 ML, the expansion increases up to 2.59% when the coverage increases to full monolayer (1.00 ML). Compared to hydrogen adsorption on Ir(111) at the fcc site, the expansion at the hcp site has the largest value, it is 1.00% at the coverage of 0.25 ML for the hcp site, and the value is 3.69% as the coverage increased to 1.00 ML. One may expect that the expansion will be much larger when there is a hydrogen atom adsorbed in the subsurface compared with the pure on-surface adsorption. Figure 2 shows such large expansion structure when there is subsurface hydrogen in addition to a full monolayer of hydrogen on the surface in the fcc site. For the topmost metal interlayer, the expansion increases sharply from 8.02% to 29.51% as the subsurface hydrogen concentrations increased from 0.25 to 1.00 ML. For a coverage of $\theta > 2.0$ ML, in this paper, we do not consider it, because larger interlayer expansion will cost more energy, which will prevent the formation of H/Ir structures of higher coverage. We can understand this conclusion from the result shown in Table 2 that the binding energy E arrives at its maximum at $\theta = 1.25$ for both the fcc plus tetra-I and hcp plus octa sites. Now turning to the H−Ir bond length d_{HIr} at different hydrogen coverage, we can know from Table 3 that for both fcc and top adsorption the H−Ir bond length varies very little with increasing θ. In particular, the calculated results of d_{HIr} for the top site vary only within an amplitude of 0.01 Å with the coverage from 0.25 ML to 1.00 ML. Note that the value of d_{HIr} for H on the top site is the shortest among that of H on fcc, hcp and bridge, the shortest bond length d_{HIr} implies a strong interaction between H and Ir atoms on the top site.

The electronic properties of H/Ir system have also been investigated in order to understand the chemical bonding of the chemisorption system. The PDOS plots for pure on-surface adsorption of hydrogen with 0.25 ML coverage at fcc, hcp, bridge, and top site are shown in Figure 3. A full monolayer of hydrogen on the surface in the fcc site plus subsurface hydrogen atom in the tetra-I site are shown in Figure 4. For comparison, the PDOS for Ir atom near the E_f in the clean surface is shown in Figure 5. It mainly consists of Ir 5d orbitals and expands
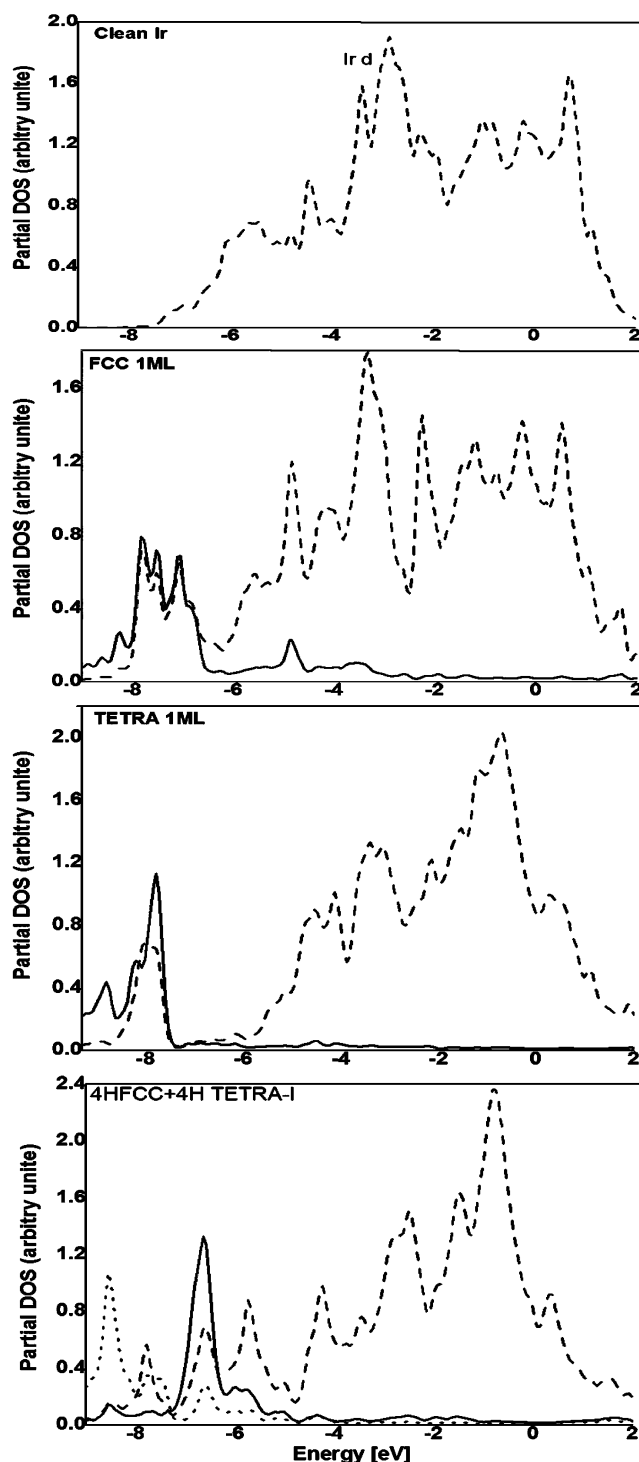

Figure 5. PDOS for (a) pure Ir(111) surface, (b) pure on-surface with four hydrogen atoms on fcc site, and (c) pure subsurface with four hydrogen atoms in tetra-I site and (d) for a full fcc site monolayer plus four subsurface hydrogen atoms in the tetra-I site. Dash lines denote Ir 5d, solid lines are on-surface H atom, dot line denotes subsurface H atom.

into a rather wide energy region from −8 to +2 eV with respect to Fermi energy. It has considerable peaks at Fermi energy. Compared to Figure 5, it can be found that the PDOS for Ir with 0.25 ML H coverage is very similar with that of clean surface. However, there is pronounced overlap of H s and Ir 5d states in the range of −8.0 to −4.0 eV, where partial electron transfer from H atoms to the Ir(111) substrate induces an outward pointing surface dipole moment and results in a small

TABLE 4: Comparing Calculated Data for On-Surface Hydrogen on Ir(111) to Hydrogen on Other Transition Metals in the (111) Surface with a Coverage of 0.25 ML on the Most Favorable Adsorption Site[a]

metal	BE	DB	h	ΔΦ			DE	
				fcc	hcp	top	calculated (PW91)	experimental
Ir (our work)	2.71 top)	0.09	1.68 (top)	−0.02	−0.01	−0.03	0.96	0.55[b]
Ir	2.74[c] (top)	0.13[c]	1.59[c] (top)			−0.04[c]	0.91[c]	
Rh	2.62 (fcc)[d]	0.11[c]	0.98[d] (fcc)	0.01[c]	0.02[c]		1.06[c]	0.81[f]
Co	2.89 (fcc)[c]	0.16[c]	0.95[c] (fcc)	−0.04[c]	0.03[c]		1.21[c]	0.69[h]
Ni	2.89 (fcc)[e]	0.14[c]	0.90[c] (fcc)	0.02[c]	0.05[c]		1.22[c]	0.98[g]
Pd	2.68 (fcc)[c]	0.15[c]	0.78[c] (fcc)	0.04[c]	0.05[c]		1.19[c]	0.90[c]
Pt	2.55 (fcc)[c]	0.04[c]	0.84[c] (fcc)	−0.06[c]	−0.06[c]	−0.16[c]	0.88[c]	0.69[c]

[a] All energies are reported in eV, adsorbed height in Å. BE is binding energy, DB is diffusion barriers, h is adsorbed height, ΔΦ is work-function change, DE is desorption energies. [b] Reference 25. [c] Reference 12. [d] Reference 26. [e] Reference 11. [f] Reference 27. [g] Reference 28. [h] Reference 29.

decrease in the work function of 0.02 eV (see Table 4). Such a broad range of overlap also shows a kind of delocalization nature of H adsorption on the Ir(111) surface. The preference of hydrogen for the atop site can be explained by comparing the hydrogen s-bands with the iridium d-bands for various adsorption configurations; the orbital overlap between these bands in the atop configuration shows a more extensive hybridization around −4.5 eV, compared to that of the fcc configuration around −7.5 eV. When the H coverage increased to 1.00 ML for pure on-surface at fcc site (see Figure 5, FCC 1 ML), there is an evident change in the PDOS of the Ir atom. All of the peaks are shifted downward about 0.5 eV compared with the clean surface, and prominent new peaks appear at about −7.0, −7.5, and −8.0 eV. Also, there is strong bonding between H and Ir at these new peaks. We can also discern that the delocalization decreases as the H coverage increased to 1.00 ML. This mainly comes from the electrostatic repulsion between hydrogen atoms. When the H coverage further increased to more than 1.0 ML with the H in mix-structures, fcc plus tetra1, the PDOS for the 1.0 ML H on-surface and 0.25, 0.50, 0.75, and 1.0 ML H in subsurface at the tetra1 site are shown in the panel labeled 4H FCC+4H TETRA-I in Figure 5. It can be seen that, with incorporation of subsurface H, the visible hybridization mainly appears in the range of −9.0 to −5.0 eV, with peaks near −6.0, −6.9, −7.5, and −8.4 eV. As the subsurface hydrogen increased to 0.5 ML, the strong overlap peaks manifest at −7.1 and −8.7 eV, with the hybridization at −7.1 eV mainly comes from the on surface hydrogen atom, and that at −8.7 eV from the subsurface hydrogen.

Meanwhile, we compare hydrogen adsorption on Ir with that of H on other transition metals (Co, Rh, Ni, Pt, and Pd)[8−12] in Table 4. Co and Rh are in the same column with Ir in the periodic table, whereas Ni, Pt, and Pd are in the column on the right. It can be seen that the variation of the binding energy on these transition metal surfaces is modest and less than 0.39 eV. For H adsorption on Ni, Pd, and Pt, the fcc site is most preferred. The adsorption energy decreases with increasing periodic number (from 4 to 6). However, in the column of Co, Rh, and Ir, there is no such trend for the variation of adsorption energy, and the preferred site is also different. In addition, hydrogen adsorption on Ir(111) shows some delocalized nature; it indicates that a weak H−H interaction occurs when there is hydrogen adsorption on Ir(111) at the fcc site. When the PES for H−Pt and H−Pd are compared, we find that the PES of H−Ir is different from those of H−Pt and H−Pd presented by Nobuhara.[30,31]

The PES for H atom penetration into the subsurface from the on-surface fcc, hcp, and top sites on Ir(111) at 0.25 ML is computed and is shown as a function of the surface normal
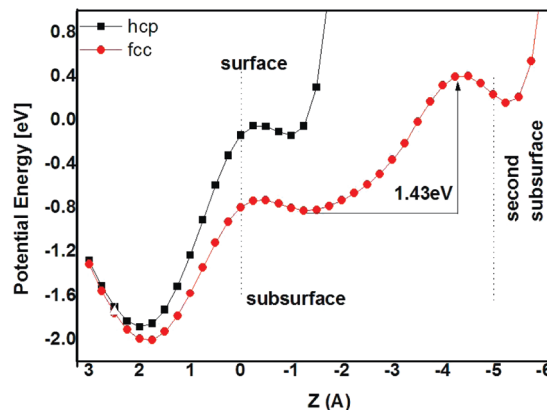

Figure 6. Calculated potential energy for the H atom at the fcc and hcp sites on Ir(111) as a function of the surface normal coordinate of the H atom with respect to the first layer z.

coordinate of the H atom with respect to the first layer z in Figure 6 (the result for the top site is not shown in this figure). Our PES studies are similar with the conclusion from Nobuhara et al.[32] They found that the energy barriers between the adjacent high symmetry sites are very small, and the low energy wave functions are positioned/centered around the top site and exhibit delocalized features. By combining the adsorption energy on the surface and subsurface with the potential energy of H diffusion into the subsurface, we discuss the diffusion path of H. When H is on the surface, it binds preferentially on the top site. For H diffusion into the subsurface, H diffuses first from the top site to the hollow site, and then incorporates into the subsurface via hollow channel. Specifically, the barrier for on-surface hydrogen from the fcc site to the octa site is 1.26 eV, whereas the barrier from the hcp site to the tetra-I site is 1.83 eV. Hydrogen diffusion from first subsurface octa site into the second subsurface region via a hollow channel is 1.43 eV. We also obtained the desorption energy 0.96 eV for hydrogen from the Ir surface at a coverage of 0.25 ML top site. The value reported by previous calculation[12] is 0.91 eV. It illustrates that our calculations within same functional (PW91) are valid. The value 0.96 eV is larger than the experimental value (0.55 eV).[25] We think this is mainly due to the unconsidered zero-point energy. If we consider the correction of zero-point energy, which is 0.18 eV for 0.25 ML coverage top site, the value of desorption energy is 0.78 eV; another reason for the difference between our calculated results and the experimental value is that the PW91-GGA DFT calculations overestimate the hydrogen-binding and -desorption energies.

4. Conclusion

In this study, periodic density functional theory calculations by using VASP code for hydrogen on the Ir(111) surface and in the Ir(111) subsurface with a wide range of coverage from 0.11 to 2.0 ML have been reported. At low hydrogen coverage ($\theta = 0.11$ ML), the binding energy of 1.97. 1.96, and 2.02 eV is found in surface fcc, hcp, and ontop sites, respectively. For all surface sites which we investigated (fcc, hcp, top, and bridge), the top site is found to be the energetically favorable site of hydrogen adsorption, with a binding energy of 2.71 eV at 0.25 ML coverage, which is in line with experimental reports. We also find that, at 0.25 ML coverage for H adsorption on Ir(111) with fcc site, the desorption energy for hydrogen from the Ir surface is 0.96 eV, the estimated value for hydrogen diffusion barrier on the surface is 0.09 eV, and the barrier for the subsurface H penetration into the second subsurface region is 1.43 eV. Compared to on-surface hydrogen adsorption, subsurface hydrogen adsorption is energetically unfavorable and takes place when on-surface hydrogen coverage is greater than a full monolayer. Compared with other transition metals, the adsorption of H on Ir(111) shows a delocalized nature. Concerning the binding ability of iridium with a hydrogen atom, it is weaker than that of hydrogen on a light transition metal such as Co and Ni, but it is evidently stronger than that of the heavy transition metals Pt, Rh and Pd.

References and Notes

(1) Chorkendorff, I.; Niemantsverdriet, H. *Concepts of Modern Catalysis and Kinetics*; Wiley-VCH: Weinheim, Germany, 2003.
(2) Faglioni, F.; Goddard, W. A., III. *J. Chem. Phys.* **2005**, *122*, 014704.
(3) Chen, W.; Ermanoski, I.; Madey, T. E. *J. Am. Chem. Soc.* **2005**, *127*, 5014.
(4) Zhang, H.; Soon, A.; Delley, B.; Stampfl, C. *Phys. Rev. B* **2008**, *78*, 045436.
(5) Nishijima, M.; Okuyama, H.; Takagi, N.; Aruga, T.; Brenig, W. *Surf. Sci. Rep.* **2005**, *57*, 113.
(6) He, Y. B.; Stierle, A.; Li, W. X.; Farkas, A.; Kasper, N.; Over, H. *J. Phys. Chem. C* **2008**, *112*, 11946.
(7) Lober, R.; Hennig, D. *Phys. Rev. B* **1997**, *55*, 4761.
(8) Nobuhara, K.; Nakanishi, H.; Kasai, H.; Okiji, A. *J. Appl. Phys.* **2000**, *88*, 6897.
(9) Lee, G.; Plummer, E. W. *Phys. Rev. B: Condens. Matter Mater. Phys.* **2000**, *62*, 1651.
(10) Lai, W. Z.; Xie, D. Q. *Surf. Sci.* **2004**, *550*, 15.
(11) Greeley, J.; Mavrikakis, M. *Surf. Sci.* **2003**, *540*, 215.
(12) Greeley, J.; Mavrikakis, M. *J. Phys. Chem. B* **2005**, *109*, 3460.
(13) Nishijima, M.; et al. *Surf. Sci. Rep.* **2005**, *57*, 113.
(14) Hagedorn, C. J.; Weiss, M. J.; Weinberg, W. H. *Phys. Rev. B* **1999**, *60*, R14016.
(15) Kresse, G.; Hafner, *J. Phys. Rev. B* **1993**, *47*, 55. Kresse, G.; Hafner, J. *Phys. Rev. B* **1994**, *49*, 14251.
(16) Kresse, G.; Furthmüller, *J. Comput. Mater. Sci.* **1996**, *6*, 15.
(17) Kresse, G.; Furthmüller, *J. Phys. Rev. B* **1996**, *54*, 11169.
(18) Perdew, J. P.; Chevary, J. A.; Vosko, S. H.; Jackson, K. A.; Pederson, M. R.; Singh; Fiolhais, D. J., C. *Phys. Rev. B* **1992**, *46*, 6671.
(19) Scheffler, M.; Stampfl, C. Theory of adsorption on metal substrates. In *Handbook of Surface Science, Vol. 2. Electronic Structure*; Horn, K., Scheffler, M., Eds.; Elsevier: Amsterdam, 2000; pp 286−357.
(20) Wanson, L. W.; Strayer, R. W. *J. Chem. Phys.* **1968**, *48*, 2421.
(21) Kittel, C. *Introduction to Solid State Physics*; Wiley: New York, 1986.
(22) Krekelberg, W. P.; Greeley, J.; Mavrikakis, M. *J. Phys. Chem. B* **2004**, *108*, 987.
(23) Ferrin, P. A.; Kandoi, S.; Zhang, J.; Adzic, R.; Mavrikakis, M. *J. Phys. Chem. C* **2009**, *113*, 1411.
(24) Chan, C. M.; Cunningham, S. L.; Van Hove, M. A.; Weinberg, W. H.; Withrow, S. P. *Surf. Sci.* **1977**, *66*, 394.
(25) Engstrom, J. R.; Tsai, W.; Weinberg, W. H. *J. Chem. Phys.* **1987**, *87*, 3104.
(26) Mavrikakis, M.; Rempel, J.; Greeley, J. *J. Chem. Phys.* **2002**, *117*, 6738.
(27) Yates, J. T.; Thiel, P. A.; Weinberg, W. H. *Surf. Sci.* **1979**, 427.
(28) Lapujoulade, J.; Neil, K. S. *J. Chem. Phys.* **1972**, *57*, 3535.
(29) Bridge, M. E.; Comrie, C. M.; Lambert, R. M. *J. Catal.* **1979**, *58*, 28.
(30) Nobuhara, K.; Nakanishi, H.; Kasai, H. *J. Appl. Phys.* **2000**, *88*, 6897.
(31) Dong, W.; Ledentu, V.; Sautet, Ph.; Eichler, A.; Hafner, *J. Surf. Sci.* **1998**, *411*, 12.
(32) Nobuhara, K.; Kasai, H.; Nakanishi, H.; Agerico, D. W. *J. Appl. Phys.* **2004**, *96*, 5020.